Microelectrode study of pore size, ion size, and solvent effects on the charge/discharge behavior of microporous carbons for electrical double-layer capacitors

Rongying Lin, Pierre-Louis Taberna, John Chmiola, Daniel Guay, Yury Gogotsi, Patrice Simon

Microelectrode Study of Pore Size, Ion Size, and Solvent Effects on the Charge/Discharge Behavior of Microporous Carbons for Electrical Double-Layer Capacitors

R. Lin,[a] P. L. Taberna,[a] J. Chmiola,[b,*] D. Guay,[c,] Y. Gogotsi,[b,**] and P. Simon[a,**,z]**

[a]*Université Paul Sabatier, Centre Inter-universitaire de Recherche et d'Ingénierie des Matériaux, Unité Mixte de Recherche CNRS 5085, France*
[b]*Department of Materials Science and Engineering and A. J. Drexel Nanotechnology Institute, Drexel University, Philadelphia, Pennsylvania 19104, USA*
[c]*Institut National de la Recherche Scientifique-Énergie, Matériaux et Télécommunications, Varennes, Quebec, J3X 1S2, Canada*

The capacitive behavior of TiC-derived carbon powders in two different electrolytes, NEt_4BF_4 in acetonitrile (AN) and NEt_4BF_4 in propylene carbonate (PC), was studied using the cavity microelectrode (CME) technique. Comparisons of the cyclic voltammograms recorded at 10–1000 mV/s enabled correlation between adsorbed ion sizes and pore sizes, which is important for understanding the electrochemical capacitive behavior of carbon electrodes for electrical double-layer capacitor applications. The CME technique also allows a fast selection of carbon electrodes with matching pore sizes (different sizes are needed for the negative and positive electrodes) for the respective electrolyte system. Comparison of electrochemical capacitive behavior of the same salt, NEt_4BF_4, in different solvents, PC and AN, has shown that different pore sizes are required for different solvents, because only partial desolvation of ions occurs during the double-layer charging. Squeezing partially solvated ions into subnanometer pores, which are close to the desolvated ion size, may lead to distortion of the shape of cyclic voltammograms.

Global warming, as well as the increasing price and decreasing availability of fossil fuels, all highlight the need to move toward a sustainable development where renewable energy and electric/hybrid vehicle engines are widely used. Renewable energy sources such as sunlight, wind, or hydro (rivers, waves, etc.) generate electrical energy which must be stored for use in autonomous systems such as transportation or electronics. Therefore, the development of high-performance electrical-energy storage devices is required.

There are two major types of electrical-energy storage devices, batteries and electrical double-layer capacitors (EDLCs). Batteries are electrochemical-energy storage devices that can be fully discharged in a few minutes or hours efficiently. Li-ion batteries, for example, exhibit high specific energy ($\sim$150 Wh/kg) but are today limited in high-power delivery/uptake as well as in low-temperature operation (failure below $-20°C$) and cycle life.[1] EDLCs, also known as supercapacitors or ultracapacitors, can be reversibly charged/discharged at higher rates as compared to batteries, thus enabling energy recovery (harvesting) at much higher rates as well.[2,3] Their cycle life ($>$500,000 cycles) as well as low-temperature operation (down to $-40°C$) positively compare to batteries. However, the specific energy of supercapacitors is about 20 times less than that of Li-ion batteries. EDLCs thus have to be used complementary with batteries in many of the applications where high-power delivery/uptake is needed, such as in hybrid electric vehicles, photo and video cameras, cell phones, etc.[3]

Recent publications suggested that a real breakthrough in improving the specific energy of EDLCs could be obtained using tailored microporous carbons[4] such as carbide-derived carbons (CDCs).[5] CDCs are obtained by the extraction of a metal from its carbide at high temperatures.[6-8] Using TiC as the precursor and chlorine as the reacting gas, CDCs with unimodal pore-size distribution and a tailored pore size ranging from 0.6 to 1.1 nm were prepared and tested in several organic electrolytes in supercapacitor cells.[9-12] Using 1.5 M tetraethylammonium tetrafluoroborate (NEt_4BF_4) in acetonitrile (AN) electrolyte, it was shown that pore sizes less than 1 nm were greatly contributing to the capacitance, suggesting that solvated ions were capable of at least partially removing their solvation shell to enter such small pores, which led to a higher capacitance.[5] Careful control of both the positive and negative electrode potentials showed that the capacitance change vs pore size exhibited two different maxima depending on the electrode polarity.[13] This was explained by the difference in size of the partially desolvated cation and anion adsorbed at the negative and positive electrode, respectively. These results also support a previous study from Kaneko's group that revealed a confinement of solvation ion in nanospace.[14] Such confinement led to a decrease in the coordination number of solvent molecules, thus shortening the distance between ions and pore walls.[14] All these results highlighted the need to adapt the electrode pore size to the electrolyte ions size for maximizing the capacitance and thus the specific energy.

Experiments carried out in solvent-free electrolytes also support these results, with capacitance as high as 150 F/g in ethyl-methyl Immidazolium-bistrifluoro-methane-sulfonylimide ionic liquid;[15] such values are comparable to those obtained in solvated electrolytes.[5] Moreover, the maximum capacitance was obtained at a pore size close to the corresponding ion size (0.7 nm in this case), suggesting that there was no room to accommodate more than one ion per pore.[15] This set of results[5,13,15] has led to a new model of the charge-storage mechanism in such nanoporous materials, in which the traditional double-layer model (solvated ions adsorbed on each pore wall) was replaced with ions lining up in the pores[16] to form an electric wire in the cylinder capacitor.

These results have demonstrated that the porous carbon/electrolyte couple must be carefully selected to maximize the capacitance. However, taking into account the possible multiple carbon/electrolyte combinations, it is important to use an electrochemical technique for characterizing active materials (carbon powders) in various electrolytes that could give information about the carbon surface/electrolyte interactions with no influence of binders, separators, current collectors, and other components of conventional electrochemical cells that can obscure the fine features of carbon–electrolyte interactions. Moreover, in such conventional cells, the electrochemical interface between the electrode and the electrolyte is large, leading to large current and thus large ohmic drop and cyclic voltammograms (CVs) that are distorted when usual scan rates (from fractions of millivolts per second up to tens of millivolts per second) are used. This ohmic drop issue hinders the study of fast

* Electrochemical Society Student Member.
** Electrochemical Society Active Member.
z E-mail: simon@chimie.ups-tlse.fr

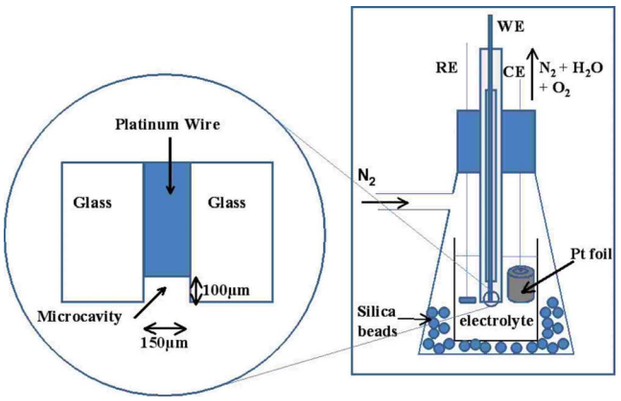

Figure 1. (Color online) Schematic of the CME electrode setup.

electrochemical processes. Moreover, time-consuming experiments are also required to perform material characterization within the full potential scan range at reduced scan rates.

Cachet-Vivier et al.[17] reported an electrochemical study of powder materials by means of the cavity microelectrode (CME). Such an electrode allows the characterization of a small amount of powder (hundreds of micrograms, depending on the size of the cavity) at a high scan rate (>50 mV/s).[18] As compared with conventional electrodes, the real electrochemical interface area is around a fraction of square millimeters and the ohmic drop arising from the bulk of the electrolyte can be neglected, allowing the use of scan rates of a few volts per second[17,19] to characterize the powder electrode. Equally important, the amount of time required to prepare and test an electrode is on the order of minutes instead of hours to days with a conventional electrode. Accordingly, CME testing is much faster than testing using conventional electrodes, enabling combinatorial electrochemistry studies.[17,19]

In this paper, we show that the use of a CME combined with CDCs of different pore sizes allows deeper insights to the double-layer capacitive charging.

Experimental

TiC powders (Alfa Aesar #40178, particle size 2 μm) were chlorinated at 500, 600, 700, and 900°C in a horizontal tube furnace. Details of the chlorination technique have been previously reported.[5] Residual chlorine and chlorides trapped in pores were removed by annealing in hydrogen for 2 h at 600°C.[20]

Argon sorption was conducted from a relative pressure, P/P_0, of 10^{-6} to 1 to assess porosity and surface-area data. Porosity analysis was carried out at liquid-nitrogen temperature, −195.8°C, on samples outgassed for at least 12 h at 300°C using a Quantachrome Autosorb-1. All isotherms are type I showing CDC to be microporous, according to the IUPAC classification. At 1000°C chlorination temperature, there is a slight hysteresis showing a small amount of mesoporosity. Pore size distributions were calculated from Ar adsorption data using the nonlocal density functional theory method provided by Quantachrome data reduction software version 1.27, and the specific surface area ($m^2\ g^{-1}$) was calculated using the Brunauer, Emmett, and Teller (BET) method.

Table I. Characteristics of CDC samples.

Chlorination temperature (°C)	BET SSA (m^2/g)	Pore volume (cm^3/g)	Average pore width (nm)	Maximum pore width[a] (nm)
500	1140	0.50	0.68	1.18
600	1269	0.60	0.74	1.23
700	1401	0.66	0.76	1.41
900	1625	0.81	1.0	2.50

[a] 85% of pore volume is below this size.

The microelectrode consisted of a Pt wire sealed in a glass rod (Fig. 1). A microcavity of $\sim 10^{-6}$ cm^3 (characteristic length of the electrode about 100 μm) was made by dissolving Pt wire in aqua regia. The microcavity was filled with active materiel by pressing it on the carbon powder spread on a glass plate; cavity cleaning was achieved by soaking the electrode in alcohol in an ultrasonic bath after each experiment. The counter electrode was a rolled platinum foil of 1 cm^2; a silver rod was used as a quasi-reference electrode. The electrochemical cell was assembled and tested in a glove box under Ar atmosphere (oxygen and water content lower than 1 ppm). All the experiments using CME have been made three times for the same sample to check reliability. All the obtained results were found to be fully reproducible. Two different electrolytes were tested, (*i*) 1.5 M NEt_4BF_4 (Acros Organics, CAS #429-06-1) in acetonitrile (Acros Organics, CAS #75-05-8, $H_2O < 10$ ppm) and (*ii*) 1 M NEt_4BF_4 (Acros Organics, CAS #429-06-1) in propylene carbonate (PC) (Acros Organics, CAS #108-32-7). Different salt concentrations were used in PC and AN to maximize ionic conductivity. CV experiments were done from 10 mV/s to 1 V/s using a multichannel potentiostat/galvanostat (VMP3, Biologic).

Results and Discussion

Table I shows the characteristics of CDC samples prepared at 500, 600, 700, and 900°C. The average pore size ranges from 0.68 to 1 nm depending on the synthesis temperature; the higher the temperature, the larger the pore size.

Table II presents the characteristics of the electrolytes used. The conductivity of the AN-based electrolyte is higher than the PC-based electrolyte due to a higher ion mobility. It is also important to note a smaller solvated size of ions in the AN-based electrolyte.

Selection of the scan rate.— Figure 2a shows the CVs of the 900°C CDC sample at scan rates from 20 to 1000 mV/s in 1.5 M NEt_4BF_4 in AN electrolyte; the current (I) has been normalized by the scan rate (v) for comparison purposes. The potential range was

Table II. Characteristics of the electrolytes studied.

Electrolyte	Electrochemical potential window (V)	Size of ions (nm) BARE[13,23] Cations	BARE[13,23] Anions	Solvated[23] Cations	Solvated[23] Anions	Conductivity ($mS\ cm^{-1}$)
1.5 M NEt_4BF_4 in ACN	−1.3 to 1.0	0.67	0.48	1.30	1.16	60
1.0 M NEt_4BF_4 in PC	−1.5 to 1.1			1.35	1.40	13

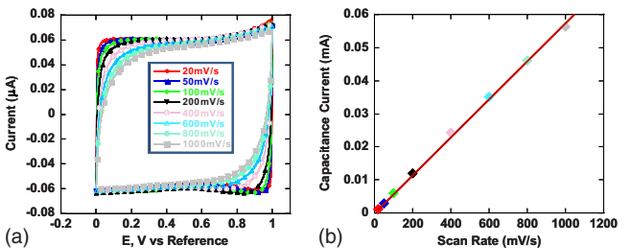

Figure 2. (Color online) Normalized CVs of the 900°C CDC sample in AN + 1.5 M NEt_4BF_4 electrolyte between 0 and +1.3 V/Ref at a scan rate from 20 to 1000 mV/s (a) and the current vs scan-rate plot (b). Currents were measured at the middle of the plateau at 0.5 V/Ref.

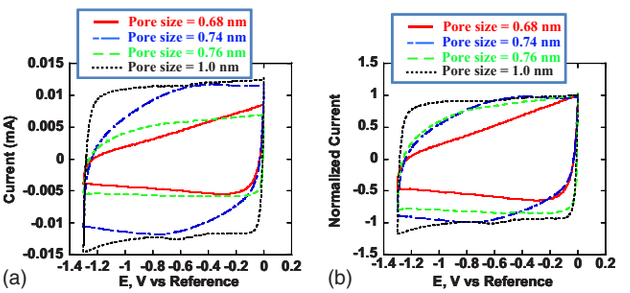

Figure 4. (Color online) CVs of CDC samples in AN + 1.5 M NEt_4BF_4 electrolyte between OCV and −1.3 V/Ref at a scan rate of 100 mV/s (a) and normalized CVs of the same samples (b).

fixed between 0 and 1 V/Ref. All the CVs exhibit a rectangular shape, associated with a pure capacitive behavior.[21] When the scan rate was increased to a high value (600 mV/s to 1 V/s), the capacitive behavior was preserved, but CVs were slightly distorted when the potential scan was reversed. Although there were some distortions, the perfect symmetry in the distortion strongly suggests that it was due to the increasing ohmic drop in the bulk electrolyte with increasing scan rate.[21] Also, for the CME, scan rates approximately an order of magnitude larger could be used without the distortion usually seen in conventional cells. Figure 2b shows the plot of the capacitive current (i.e., the current value at the plateau observed in the CVs) change vs the scan rate. A perfect linear plot can be seen, thus confirming that the currents measured from the CV experiments are purely capacitive. From these results, it appears that a potential scan rate of 100 mV/s combines a fast data-acquisition rate together with a negligible ohmic drop in the electrolyte bulk, allowing the observation of a pure capacitive behavior for the CDC tested, in agreement with our previous study.[19] This scan rate was used in the majority of experiments reported in this article.

1 M NEt_4BF_4 in AN electrolyte

Cyclic voltammetry.— Figure 3a shows the CVs of various CDC samples at 100 mV/s in a 1.5 M NEt_4BF_4 in AN electrolyte at 25°C, between the rest potential of the CME up to positive potential values. The rest potential is the zero-current potential, also denoted as the open-circuit voltage (OCV). All of the CVs exhibit the previous rectangular shape characteristic of purely capacitive behavior. In these experiments, charging of the electrochemical double layer is carried out during the positive scan from 0 up to 1 V/Ref, while double-layer capacitance discharge occurs during the reverse potential scan, from +1 down to 0 V/Ref. The potential range explored is always higher than the OCV; all electrodes are kept positively charged during the whole scan. Accordingly, the charge/discharge of the double layer is mainly achieved with the adsorption/desorption of the anions of the electrolyte, i.e., BF_4^- ions.[22] The capacitive

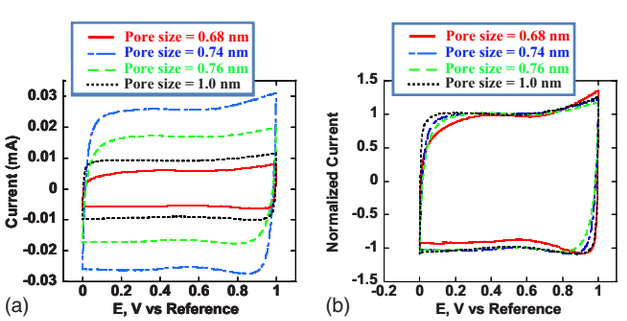

Figure 3. (Color online) CVs of the four CDC samples in AN + 1.5 M NEt_4BF_4 electrolyte between OCV (0 V/Ref) and +1 V/Ref. Scan rate: 100 mV/s (a) and normalized CVs of the same samples (b).

current differs from one sample to another because (*i*) the powder weight in the CME cannot be kept exactly the same from one experiment to another, though data averaged over a number of tests represents the behavior of the materials well,[19] and (*ii*) the specific capacitance is different for every sample. This difference in the capacitive currents makes the direct comparison of the sample based on CV shape difficult. Accordingly, all current values (*I*) have been normalized to the current value measured at 0.45 V/Ref during the charge, i.e., in the pure capacitive behavior region. By doing this, we normalized the linear region of all the electrode CVs to the same capacitance; the shape of the CVs is preserved, but comparisons become easier. The normalized plot is presented in Fig. 3b. According to Table I, the pore size of the carbon samples increased from 0.68 to 1 nm when the synthesis temperature was increased from 500 to 900°C. Because no major difference can be seen in Fig. 3b, BF_4^- ion adsorption/desorption onto the carbon surface seems not to be limited; the carbon pore size is large enough to accommodate BF_4^- ions (desolvated size is 0.48 nm,[13] solvated size of $BF_4^-{\cdot}9AN$ is 1.16 nm[23]) inside pores of all four CDCs studied.

Figure 4a shows the CVs of CDC samples from the OCV down to negative potentials (−1.3 V/Ref) at a scan rate of 100 mV/s. Here, all samples were negatively charged within the whole potential window. Charge (from 0 down to −1.3 V/Ref) and discharge (from −1.3 up to 0 V/Ref) of the double layer was mainly achieved with the NEt_4^+ cations.[22] Current values were normalized to a constant value on discharge in Fig. 4b, as they were for positive polarizations. Qualitatively, based on the shape of their CVs, the electrochemical behavior of the CDCs was different depending on the synthesis temperatures. The 1 nm sample (900°C) exhibited pure capacitive behavior with a rectangular-shaped CV. However, when the synthesis temperature (and thus the pore size) was decreased, the CVs became more distorted. This shift from purely capacitive behavior was clearly visible during the discharge scan (between −1.3 and −0.6 V/Ref), where the current response for a given potential was largely decreased (0.74 and 0.68 nm samples). The CV of the 500°C sample with the smallest pore size was most distorted. Here, the capacitance changed with the applied potential. On charge, during the negative potential scan, the current decreased constantly, while the increase in current was much more pronounced on the reverse scan, leading to an asymmetric CV. This behavior is far from the one expected for the capacitive charge/discharge of the electrochemical double layer.

Figure 5a shows the CVs of the four CDC samples in 1.5 M NEt_4BF_4 in AN electrolyte between −1.3 and +1 V/Ref. All the plots were normalized in Fig. 5b to the maximum current at 1 V/Ref. In these experiments, each sample was characterized over the whole potential range, i.e., the potential scan crossed the OCV. Negative of the OCV (which was measured close to 0 V/Ref for all samples), the capacitive behavior originates from cation adsorption; positive of the OCV, it originates from anions adsorption. Two different potential ranges can be clearly identified in Fig. 5b, above and

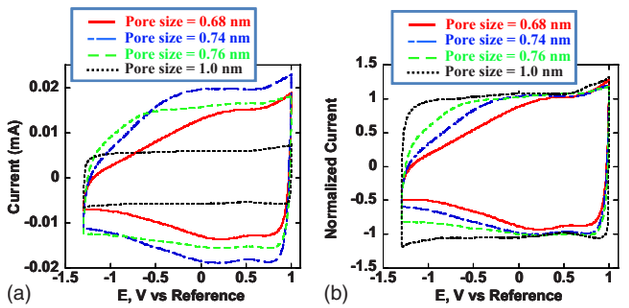

Figure 5. (Color online) CVs of CDC samples in AN + 1.5 M NEt_4BF_4 electrolyte between −1.3 and +1 V/Ref at a scan rate of 100 mV/s (a) and normalized CVs of the same samples (b).

below the OCV. For potential higher than OCV, the CVs are rectangular-shaped, typical for pure double-layer capacitive behavior. When the potential scan is reversed at 1 V/Ref to negative, only slight changes in the CVs can be observed above the OCV. This potential range corresponds to the discharge of the positive electrode, where anions are removed from the porous carbons. This inhomogeneous behavior is in good agreement with Fig. 3. When the potential scan is negative of the OCV (0 V/Ref), the rectangular shape of the CV is lost for all samples except the 1 nm sample, which has the largest pore size (1 nm). The smaller the pore size (the lower the synthesis temperature), the more distorted the CVs. This shift from purely capacitive behavior is also present when the potential scan rate is reversed at −1.3 V/Ref to positive values. These distortions of CVs were also reported by Salitra et al.[24] using a conventional three-electrode cell with an activated carbon cloth as the active material.

CV experiments were performed at a low scan rate to investigate kinetic effects on the electrochemical behavior. Figure 6 shows the CV plots recorded at 10 mV/s, i.e., a slow scan rate usually employed for electrode characterization in conventional cells. The shape of the plots is preserved even at 10 mV/s; all CVs appear to be distorted and asymmetric, except for the larger-pore-size sample (900°C). However, less distortion was observed for the 700°C CDC (0.76 nm) sample, with the shape of CV becoming closer to the

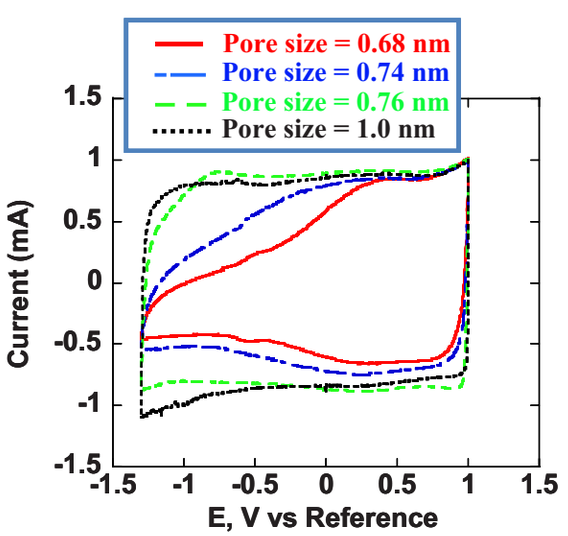

Figure 6. (Color online) Normalized CVs of CDC samples in AN + 1.5 M NEt_4BF_4 electrolyte between −1.3 and +1 V/Ref. Scan rate: 10 mV/s.

rectangular one. This suggests that kinetics does play a role in the process, leading to CV distortion for samples with pore size close to the adsorbed ion size.

BF_4^- adsorption.— The capacitive behavior of the CVs in Fig. 3b is kept the same, whatever the pore size of the carbon used, meaning that BF_4^- ion transport and adsorption is not limited in these nanopores. Maximization of the capacitance is achieved by minimizing the unoccupied volume in the porous structure of the carbon. In our experiments, pores of 1 nm, for instance, are too large, because the anion adsorptions occurs without any limitation even for a pore size of 0.68 nm. This result is in good agreement with previous work that showed, using large three-electrode cells (4 cm^2), a maximum specific capacitance for the 500°C sample (0.68 nm pore size).[13] It supports the hypothesis of ion desolvation upon adsorption in subnanometer pores, because the pore size is smaller than the solvated ion size (Table II) and fully solvated ions would not be able to enter CDC pores. However, it also shows that there is little resistance to ion adsorptions in the pores in the 0.7–1.0 nm range, suggesting a potential for developing high-power EDLC capable of a fast charge/discharge.

Et_4N^+ adsorption.— The distortion of the CVs presented in Fig. 4 and 5 for small-pore-size samples cannot be caused only by an increase of the cell series resistance when the pore size and graphitization decreases.[25] This cell series resistance combines three main contributions, the bulk electrical resistance of the CDCs, the bulk electrolyte resistance, and the electrolyte resistance in the pores of the carbon. As the electrical conductivity of CDC is in the order of tens of Siemens per centimeter,[5] i.e., a thousand times more than the ionic conductivity of the electrolyte (see Table II), this contribution can be neglected, and the increase in CV distortion observed in Fig. 4 and 5 must be linked with an increase in electrolyte resistance. However, the same trend as in Fig. 5 is observed for CV plots recorded at 10 mV/s (Fig. 6), where the ohmic drops in the electrolyte bulk are about 10 times less. Thus, the poor capacitive behavior of the small-pore-size samples was not due to CME polarization generally observed for high scan rates when the ohmic drop becomes too large.[17] Accordingly, the limitation observed is not linked with bulk electrolyte resistance or changing carbon resistance but with the ion transport in the porous carbon network (squeezing ions into small pores).

At negative polarizations, when the carbon pore size is decreased below 1 nm (900°C sample), pores start to become too narrow to efficiently accommodate the cations [1.30 and 0.67 nm with (Et_4N^+·7AN) and without the solvation shell, respectively[13,23]]. For pores equal to or smaller than 0.76 nm (700°C sample), the capacitive behavior is poor, with a huge resistive part linked to the cation-transport limitation in the pores due to a size effect. For pores ⩾1 nm, good accessibility to the carbon porous network and a pure capacitive behavior can be observed. The optimum pore size for the Et_4N^+-ion adsorption on carbon from AN electrolytes is therefore between 0.76 and 1 nm. 700°C CDC with 0.76 nm pores shows little distortion at the low rate (Fig. 6).[5] Hence, the effective size of the adsorbed ion in AN during double-layer charging/discharging can be estimated to be between 0.76 and 1 nm, some intermediate value between purely solvated and desolvated (see Table II), as is the case of positive polarizations and BF_4^- adsorption.

Taking into account the size of the solvated Et_4N^+ and BF_4^- ions in AN (1.3 and 1.16 nm, respectively), these results confirm that ions must be at least partially desolvated to enter these small pores. Previous results we obtained showed that the optimum pore size to maximize the carbon capacitance was about 0.7 and 0.8 nm for the BF_4^- and Et_4N^+ ions in AN, respectively. Results presented in Fig. 4 and 5 agree with these recent findings that were obtained in a series of experiments at 20 mV/s using large 4 cm^2 cells assembled with 60 mg of CDC but show that a resistance to cation transport exists in pores smaller than ∼0.8 nm. Because this size is fairly close to the desolvated ion size (Table II), there is a possibility that errors in

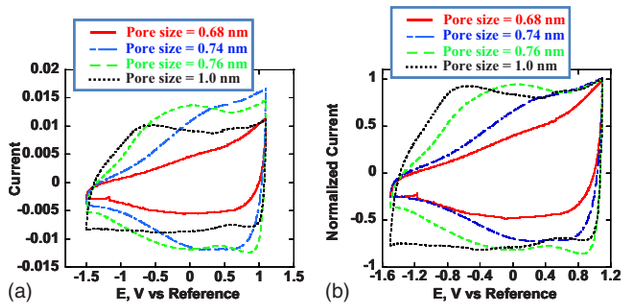

Figure 7. (Color online) CVs of the CDC samples in PC + 1 M NEt_4BF_4 electrolyte between −1.5 and +1 V/Ref (a) and normalized CVs of the same samples (b). Scan rate: 100 mV/s.

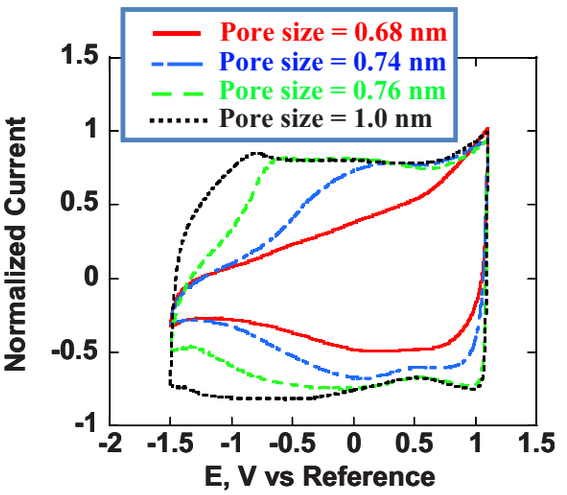

Figure 8. (Color online) Normalized CVs of the CDC samples in PC + 1.0 M NEt_4BF_4 electrolyte between −1.3 and +1 V/Ref. Scan rate:10 mV/s.

the average pore-size measurement may lead to overestimation of the pore size and that the real pore size is somewhat smaller, too close to the ion dimensions. It is also expected that bottlenecks exist between pores. Thus, even if the average pore size of 0.7 nm would be sufficient to accommodate a NEt_4^+, a material with a larger pore size is needed to ensure that bottlenecks connecting the pores allow ions to pass through. Finally, we do not know the distance between the ion and the pore wall that would provide the minimum energy. This can also lead to the pore size being larger than the ion size. However, if the assumption of complete desolvation of ions upon double-layer charging is correct, the electrode behavior should be solvent independent, because no solvent enters the pores. To prove this hypothesis, CDC samples have been characterized using the same technique in the 1 M NEt_4BF_4 in PC electrolyte.

1 M NEt_4BF_4 in PC.— Figure 7a shows the CVs of various carbon samples between −1.5 and 1 V/Ref at 100 mV/s. OCV values were measured between +0.3 and +0.5 V/Ref, depending on the sample studied. This figure is similar to Fig. 5a, with the potential scan crossing the OCV. All the plots have been normalized in Fig. 7b at the maximum current at 1 V/Ref.

In the +0.3 to + 1 V/Ref potential range (above the OCV) where the anion adsorption occurs, larger-pore-size samples (1 and 0.76 nm, respectively, for 900 and 700°C) exhibit a capacitive behavior. The small-pore-size carbons (0.74 and 0.68 nm, respectively, for 600 and 500°C) show a different electrochemical response, with an asymmetric distortion of the rectangular-shape CV, indicating a shift from a pure capacitive behavior. Similar distorted CVs were observed for activated carbon-cloth electrodes in the same electrolyte,[24] confirming that the observed behavior is not an artifact of using CME. If we compare these results with Fig. 5, the optimum pore size for the anion adsorption is here shifted to somewhat larger values, i.e., from ≤0.68 nm in AN up to about ~0.75 nm in PC-based electrolyte. This means that the size of the adsorbed BF_4^- anion in a PC-based solution is larger than in AN-based electrolytes, in agreement with previous studies,[9] suggesting that only partial desolvation of ions occurs in pores and that a stronger ion-solvent interaction exists in the case of PC.

In the 0 to − 1.5 V/Ref potential range, the electrochemical signature is different from one sample to another. The current in this potential range is mainly due to cation adsorption (negative scan) and desorption (positive scan). All the plots are distorted, and none presents typical capacitive behavior, such as presented in Fig. 3. The smaller the pore size, the lower the current for a given potential. Interestingly, even the large-pore-size sample CV (900°C) fails to show a pure electrochemical capacitive signature. When PC is used instead of AN, the optimum pore size shifts to a larger value. These results are in good agreement with the calculated solvated sizes of BF_4^-·8PC and NEt_4^+·4PC[23] that are 1.40 and 1.35 nm, respectively (Table II).

Similar to tests in AN, CV experiments in PC were made at a low scan rate of 10 mV/s (Fig. 8) to check if the electrochemical behavior would change. As previously observed in AN-based electrolyte, the asymmetric shape of the plots was preserved, thus demonstrating that the poor capacitive behavior of the small-pore-size samples was not due to bulk resistance.[17]

Because we have observed a solvent effect, the accuracy of pore-size measurement[26] is not to be blamed for the observed discrepancies between the desolvated ion size and the minimal pore size producing rectangular CVs. Accordingly, we can assume that ions were partially desolvated and thus squeezed to enter into small pores. Such steric hindering could lead to an increase in resistance. Partial desolvation (a decreased number of solvent molecules in the solvation shell of an ion) has been suggested to occur in aqueous electrolytes in narrow-slit pores or nanotubes[23] and for Li^+ in organic electrolytes in porous carbons.[24] If the energy of removing the last few solvent molecules is higher than that required to remove the first molecules, partial desolvation is probable. This hypothesis is supported by the adsorbed ion size dependence on the solvent. Different solvation energies are expected for PC and AN.

All these factors highlight the difficulty to predict the optimal pore size of the carbon electrode just based on the size of a bare or solvated ion and the need to transcend conventional thinking for proper carbon–electrolyte pairing. Microelectrode studies provide a convenient means for quick measurement of the correlations between the pore size and electrode performance for a variety of carbons, electrolytes, and solvents. Such a technique combining high-rate CVs on tailored unimodal porous carbons is thus particularly well adapted to the study of the capacitive behavior of EDLC electrodes, but more generally it is useful for studying processes where ion-size/pore-size interactions play an important role, including water desalinization and/or ion exchange through porous membranes in cells.

Conclusions

A CME study of the electrochemical behavior of CDCs with a unimodal pore-size distribution and a tailored pore size ranging from 0.68 to 1 nm has shown that the size of the Et_4N^+ cation and BF_4^- anion adsorbed in carbon pores is different depending on the nature of the solvent (AN or PC). The adsorbed ion size, estimated from the CVs recorded at 100 mV/s, was found to decrease in the following sequence: Et_4N^+ in PC > Et_4N^+ in AN > BF_4^- in PC > BF_4^- in AN. When comparing the size of adsorbed ions deduced from these measurements to the solvated ion size, it appears that

ions have to be partially desolvated to enter sub-nanometer pores. However, using the CME technique, we were able to reproduce these previous results obtained over a few weeks of continuous work in a few days. More importantly, we have shown that even for the same ions, carbon electrodes with different pore sizes will be required depending on whether the maximum energy storage (capacitance) or charge/discharge rate or low energy losses in cycling are required. Moreover, different pore sizes are needed for the negative and positive electrodes. Because the ideal pore size may be neither the bare ion nor solvated ion size, it is currently impossible to predict it a priori. CME is certainly a method of choice for material screening and selecting the EDLC carbon/electrolyte couples.

Acknowledgments

J. Chmiola was supported by an NSF GRFP fellowship. Y. Gogotsi was partially funded through the Pennsylvania Nanotechnology Institute (NTI) and PA Nano grants to Y-Carbon, Inc. R. Lin was funded through the European Erasmus Mundus programme from the European Commission.

Centre National de la Recherche Scientifique assisted in meeting the publication costs of this article.

References

1. M. Armand and J. M. Tarascon, *Nature (London)*, **451**, 652 (2008).
2. J. R. Miller and P. Simon, *Science*, **321**, 651 (2008).
3. P. Simon and Y. Gogotsi, *Nature Mater.*, **7**, 845 (2008).
4. F. Beguin and E. Frackowiak, CRC Press/Taylor and Francis, Boca Raton, FL, In press.
5. J. Chmiola, G. Yushin, Y. Gogotsi, C. Portet, P. Simon, and P.-L. Taberna, *Science*, **313**, 1760 (2006).
6. R. Dash, J. Chmiola, G. Yushin, Y. Gogotsi, G. Laudisio, J. Singer, J. Fischer, and S. Kucheyev, *Carbon*, **44**, 2489 (2006).
7. Y. G. Gogotsi, I.-D. Jeon, and M. J. McNallan, *J. Mater. Chem.*, **7**, 1841 (1997).
8. Y. G. Gogotsi, K. G. Nickel, D. Bahloul-Hourlier, T. Merle-Mejean, G. E. Khomenko, and K. P. Skjerlie, *J. Mater. Chem.*, **6**, 595 (1996).
9. A. Janes, L. Permann, P. Nigu, and E. Lust, *Surf. Sci.*, **560**, 145 (2004).
10. E. Lust, A. Janes, and M. Arulepp, *J. Electroanal. Chem.*, **562**, 33 (2004).
11. A. Janes and E. Lust, *J. Electrochem. Soc.*, **153**, A113 (2006).
12. J. Leis, M. Arulepp, A. Kuura, M. Latt, and E. Lust, *Carbon*, **400**, 2122 (2006).
13. J. Chmiola, C. Largeot, P. L. Taberna, P. Simon, and Y. Gogotsi, *Angew. Chem., Int. Ed.*, **47**, 3392 (2008).
14. T. Ohkubo, T. Konishi, Y. Hattori, H. Kanoh, T. Fujikawa, and K. Kaneko, *J. Am. Chem. Soc.*, **124**, 11860 (2002).
15. C. Largeot, C. Portet, J. Chmiola, P.-L. Taberna, Y. Gogotsi, and P. Simon, *J. Am. Chem. Soc.*, **130**, 2730 (2008).
16. J. S. Huang, B. G. Sumpter, and V. Meunier, *Angew. Chem., Int. Ed.*, **47**, 520 (2008).
17. C. Cachet-Vivier, V. Vivier, C. S. Cha, J. Y. Nedelec, and L. T. Yu, *Electrochim. Acta*, **47**, 181 (2001).
18. M. Zuleta, P. Bjornbom, A. Lundblad, G. Nurk, H. Kasuk, and E. Lust, *J. Electroanal. Chem.*, **586**, 247 (2006).
19. C. Portet, J. Chmiola, Y. Gogotsi, S. Park, and K. Lyan, *Electrochim. Acta*, **53**, 7675 (2008).
20. E. N. Hoffman, G. Yushin, T. El-Raghy, Y. Gogotsi, and M. W. Barsoum, *Microporous Mesoporous Mater.*, **112**, 526 (2008).
21. B. E. Conway and W. G. Pell, *J. Power Sources*, **105**, 169 (2002).
22. S. Shiraishi, H. Kurihara, L. Shi, T. Nakayama, and A. Oya, *J. Electrochem. Soc.*, **149**, A855 (2002).
23. C. M. Yang, Y. J. Kim, M. Endo, H. Kanoh, M. Yudasaka, S. Iijima, and K. Kaneko, *J. Am. Chem. Soc.*, **129**, 20 (2007).
24. G. Salitra, A. Soffer, L. Eliad, Y. Cohen, and D. Aurback, *J. Electrochem. Soc.*, **147**, 2486 (2000).
25. B. E. Conway and W. G. Pell, *J. Power Sources*, **96**, 57 (2001).
26. G. Laudisio, R. K. Dash, J. P. Singer, G. Yushin, Y. Gogotsi, and J. E. Fischer, *Langmuir*, **22**, 8945 (2006).